Appl Nanosci (2013) 3:329–333
DOI 10.1007/s13204-012-0135-3

ORIGINAL ARTICLE

Synthesis and characterization of whisker-shaped MnO_2 nanostructure at room temperature

Deogratius Jaganyi · Mohammad Altaf · Isaac Wekesa

Received: 21 March 2012 / Accepted: 17 May 2012 / Published online: 6 June 2012

Abstract Manganese dioxide nanoparticles have been synthesized, via a facile one-step solution phase approach, by the reduction of potassium permanganate with sodium thiosulphate at room temperature. Upon addition of thiosulphate to the solution of permanganate, a transparent dark-brown color species appeared which was stable for several months. The obtained MnO_2 solution was characterized by means of UV–vis spectra, Transmission electron microscopy (TEM), and Fourier transforms infrared spectroscopy. Fourier transforms infrared spectroscopy spectra of pure MnO_2 show the occurrence of O–Mn–O vibrational mode at around 600 and 475 cm^{-1}. The chemical composition was obtained by EDX analysis and confirmed the presence of Mn and O in the sample. From the TEM image, the surface morphology of the sample shows uniformly dispersed particles, which are spherical in shape. The selected area electron diffraction patterns revealed that the MnO_2 are crystalline in nature.

Keywords Manganese dioxide nanoparticle · FT-IR · TEM

Introduction

Nanomaterials have captured the imagination of researchers lately due to the significant difference in their properties compared to the coarse-grained counterpart. Metal-oxide nanocrystals are expected to find useful applications in catalysis, energy storage, magnetic data storage, sensors, and ferrofluids (Zarur and Ying 2000; Majetich and Jin 1999; Nayral et al. 2000; Raj and Moskowitz 1990). In particular, colloidal metal-oxide nanocrystals are of great interest for technological applications owing to their unique size-dependent properties and excellent process ability. There have been numerous types of reactions that have been catalyzed using colloidal and supported metal nanocatalysts such as oxidations (Spiro and De Jesus 2000; Shiraishi and Toshima 1999; Launay et al. 1998; Akram et al. 2007; Altaf et al. 2009; Kabir-ud-Din et al. 2008; Akram et al. 2011), cross-coupling reactions (Li et al. 2002; Li and El-Sayed 2001; Narayanan and El-Sayed 2003; Kogan et al. 2002; Gopidas et al. 2003; Yeung and Crooks 2001), electron transfer reactions (Narayanan and El-Sayed 2004a, b; Sharma et al. 2003), hydrogenations (Ohde et al. 2004; Somorjai 1997; Boudjahem et al. 2004; Claus and Hofmeister 1999), fuel cell reactions (Anderson et al. 2002; Long et al. 2000; Moore et al. 2003), and many others. Numerous review articles have been published on the use of colloidal (Bradley 1994; Duff and Baiker 1995; Toshima 1996; Boennermann et al. 1996; Narayanan and El-Sayed 2004a; Mayer 2001; Bonnemann and Richards 2002; Moiseev and Vargaftik 2002) and supported (Toshima and Yonezawa 1998; Puddephatt 1999; Henry 2000; Kralik et al. 2000; Kralik and Biffis 2001; Thomas and Raja 2001; Thomas et al. 2003) transition metal nanoparticles as catalysts for a variety of organic and inorganic reactions.

As regards all other non-noble metals or transition metal oxides studied in modern times, MnO_2 is one of the most attractive inorganic materials not only because of its physical and chemical properties and wide range of applications in catalysis, ion-exchange, molecular adsorption, biosensor and particularly energy storage but also because of its low cost and environmentally benign nature.

D. Jaganyi · M. Altaf (✉) · I. Wekesa
Faculty of Science and Agriculture, School of Chemical and Physical Sciences, University of KwaZulu-Natal, Private Bag X01, Scottsville, Pietermaritzburg 3209, South Africa
e-mail: altafamu@gmail.com

Especially in catalysis, MnO_2 becomes an obvious choice as an oxidant. Solution-based synthesis and use of metal-oxide nanoparticles, however, require special mention due to their low cost, mildness, convenience and use without additional templates and apparatus. In spite of their important applications, there have been only few reports on synthesis of monodisperse colloidal manganese oxide nanoparticles (Kabir-ud-Din and Iqubal 2009; Jana et al. 2007; Khan et al. 2010). In this paper, we report a facile one-step solution phase synthetic approach of MnO_2 nanoparticles without any template or stabilizing agent.

Experimental

Materials

All chemicals were analytical grade reagents. Potassium permanganate (98.5 %, E. Merck, SA), and sodium thiosulfate (99 %, E. Merck, SA) were used as received without further purification. Ultra-pure water was used for the preparation of all reagents solutions. Permanganate solutions were stored in a dark glass bottle and standardized by titration against oxalate.

Synthesis of manganese dioxide nanoparticles

In a typical synthesis of MnO_2 nanoparticles in solution phase was carried out as follows: 0.0158 g of $KMnO_4$ was dissolved in 75 ml of ultra-pure water, and the mixture was fleetly stirred for 2 h. 0.0931 g of sodium thiosulphate dissolved in 25 ml of ultra-pure water and then it was added to the permanganate solution at room temperature. The color of the solution changed rapidly from purple to yellow–brown (indicating the onset of the formation of MnO_2 nanoparticles) and finally dark brown. The resulting solution was perfectly transparent and was very stable over extended periods of several months.

Instrumental details

UV–visible absorption spectra were obtained on UV-1800 Shimadzu spectrophotometer using 10 mm quartz cell. Transmission electron microscopy (TEM) was carried out on a JEOL-2010 transmission electron microscope operated at an accelerating voltage of 80 kV. One or two drops of the solution containing the as-synthesized composites were deposited onto the amorphous carbon film supported on a copper grid and allowed to dry at room temperature in air. EDX spectrum was obtained from Oxford, Link, ISIS 300 instrument. Fourier transform infrared (FT-IR) spectra of the samples were recorded with a Perkin Elmer BX FT-IR infrared spectrometer in the range of 4,000–400 cm^{-1}.

Results and discussion

UV–vis spectral study

In order to study the growth mechanism for the evolution of spherical MnO_2 nanoparticles, a UV–visible study was carried out. The progress of the reaction or the formation of spherical MnO_2 nanoparticle from aqueous $KMnO_4$ was monitored by a UV-1800 Shimadzu spectrophotometer measuring the changes in the specified absorbance maxima. It was observed that the intensity of charge transfer transition (at 506, 525, 545, and 566 nm) decreased gradually by addition of sodium thiosulphate solution to the aqueous solution of potassium permanganate. The purple color of $KMnO_4$ started to fade, and the color changed from purple to yellow–brown and finally to dark brown. The progress of the reaction has been accounted from a steady decrease of all the four absorbance maxima at specified band (506, 525, 545, and 566 nm) positions with increase in $[Na_2S_2O_3]$ as shown in Fig. 1. The purple color of $KMnO_4$ faded away with increase in thiosulphate concentration producing a brown coloration, indicating the progress of the reduction reaction. All the spectra cross a common isosbestic point and are shown by a circle in Fig. 1, which gives valuable information about the reaction that 1 mol of reactant is converted to 1 mol of the product and a chemical equilibrium existed between the reactant and product at a particular wavelength, 360 nm.

A broad distinctive peak was observed in the 360 nm range for a lower concentration, which is in contrast to the above-mentioned procedure for monitoring the four peaks. A significant blue shift of the adsorption edge for the as-obtained MnO_2 dispersion in comparison to bulk MnO_2 is

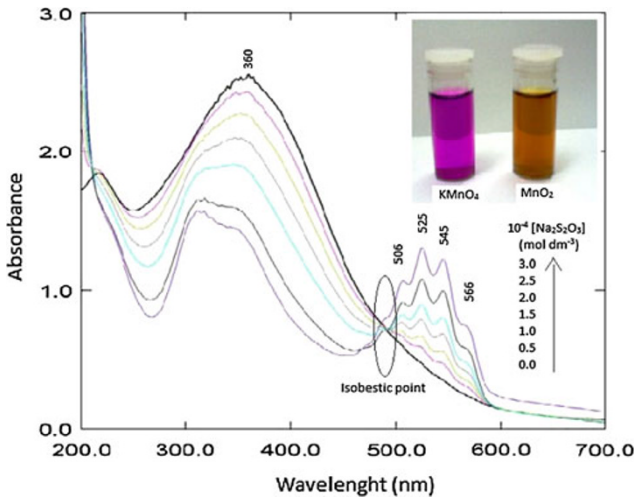

Fig. 1 UV–visible spectra of the mixtures containing a fixed amount of $KMnO_4$ (= 8.0×10^{-4} mol dm^{-3}) and varying amounts of $Na_2S_2O_3$

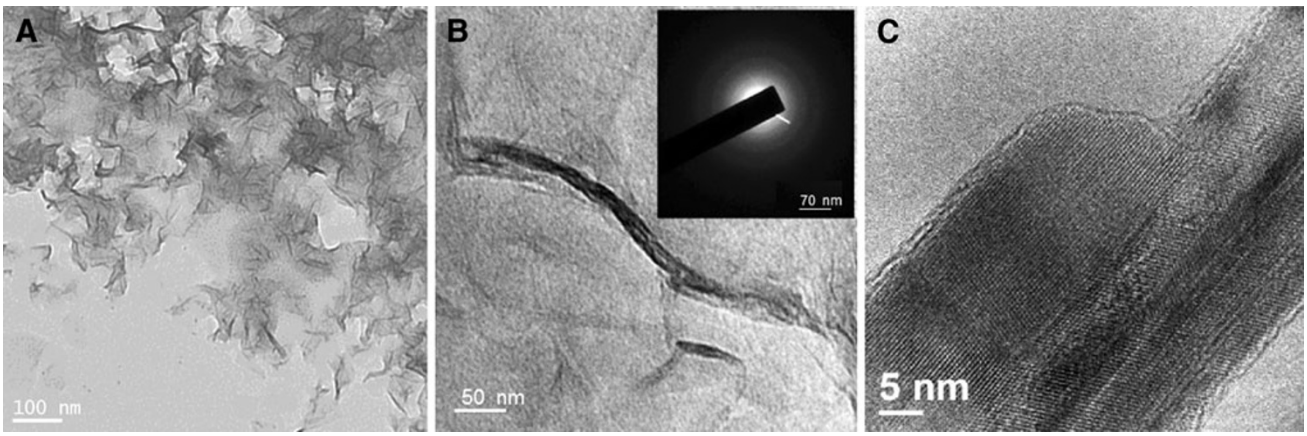

Fig. 2 **a** TEM of MnO_2 whiskers and **b** TEM of a single MnO_2 whisker and **c** HRTEM image of MnO_2 whisker and (**b** *inset*) SEAD pattern of MnO_2

Fig. 3 EDX analysis of as-synthesized MnO_2 and the elemental composition

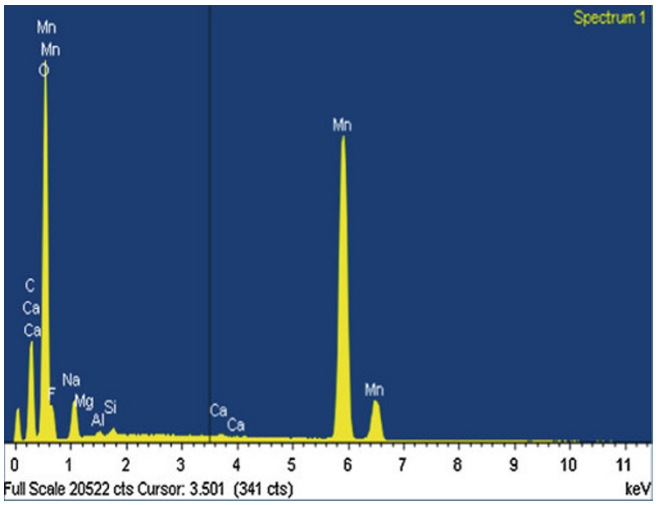

Element	Weight%
C K	20.23
O K	36.15
F K	1.97
Na K	2.91
Mg K	0.07
Al K	0.15
Si K	0.24
Ca K	0.11
Mn K	38.17
Totals	100.00

found which can be explained because of the presence of very small MnO_2 nanoparticles.

TEM study

The morphology and particle size of the product were determined from transmission electron microscopy. The observed results are given in Fig. 2a for freshly prepared manganese dioxide nanoparticles. Because of the random nature of aggregate formation, the synthesized whisker shape MnO_2 nanoparticle aggregates have a broad distribution of sizes and shapes. This variety of sizes and shapes are apparent from the TEM images. The whiskers formed are 150–200 nm in length and 10–20 nm in diameter. The HRTEM image of the single whisker, the corresponding SAED pattern, and the lattice image of the sample under the ultrasound are shown in Fig. 2b. The observed lattice spacing of 2.6 and 2.9 Å correspond to the (103) and (112) planes of MnO_2, respectively. The SAED pattern reveals the MnO_2 particles are crystalline in nature. The size of nanoparticle according to the HRTEM image was found to be about 10 nm.

The chemical composition of the nanoparticles has been analyzed using EDX analysis as shown in Fig. 3. The Cu peaks are the signal detected from the TEM grid. This result confirms the presence of Mn and O in the sample.

Fourier transforms infrared spectral study

Fourier transforms infrared (FT-IR) spectroscopy is known for its high sensitivity, especially in detecting inorganic and organic species with low content. The FT-IR spectrum is presented in Fig. 4. Two absorption bands observed at 600 and 475 cm^{-1} are corresponded to the characteristic stretching collision of O–Mn–O, which demonstrated the presence of the MnO_2 in the sample. The typical broad absorption in the wavelength ranges between 4,000 and 3,000 cm^{-1} are allocated both the stretching collision of

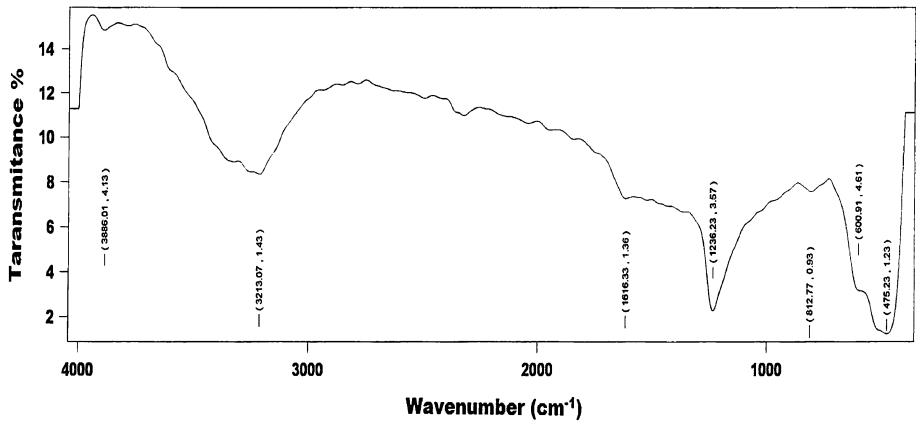

Fig. 4 FT-IR spectra of as-synthesized MnO_2 nanoparticles

H–O–H and hydroxyl absorption, while the peak detected at 1,616 cm^{-1} symbolized the bending collision of adsorbed water. The simultaneous presence of both these peaks indicated the existence of adsorbed H_2O molecule for this sample. Furthermore, the absorption peak at the wavelength near 1,236 and 812 cm^{-1} represented the surface –OH groups of Mn–OH for colloidal MnO_2 nanoparticles.

Conclusions

In summary, Manganese dioxide nanoparticles have been synthesized, via a facile one-step solution phase approach, by the reduction of potassium permanganate with sodium thiosulphate at room temperature. TEM analysis revealed the size of nanoparticles as 10 nm and polycrystalline nature of particles is also observed. This low temperature synthetic route, based on the simple reaction with no participation of catalysts or templates and requiring no expensive and precise equipment, ensures higher purity of the products, greatly reduces the production cost, and thus offers great opportunity for industry scale-up preparation of nanostructure materials.

Acknowledgments The authors thank to the University of KwaZulu-Natal for funeral support. One of the authors, Mohammad Altaf is greatful to the University of KwaZulu-Natal for the postdoctoral fellowship.

References

Akram M, Altaf M, Kabir-ud-Din (2007) Oxidation of aspartic acid by water soluble colloidal MnO_2 in absence and presence of nonionic surfactants. Indian J Chem 46A:1427–1431

Akram M, Altaf M, Kabir-ud-Din (2011) Oxidative degradation of dipeptide (glycyl-glycine) by water-soluble colloidal manganese dioxide in aqueous and micellar media. Colloids Surf B Biointerfaces 82:217–223

Altaf M, Akram M, Kabir-ud-Din (2009) Water-soluble colloidal manganese dioxide as an oxidant for L-tyrosine in the absence and presence of non-ionic surfactant TX-100. Colloids Surf B Biointerfaces 73:308–314

Anderson ML, Stroud RM, Rolison DR (2002) Enhancing the activity of fuel-cell reactions by designing three-dimensional nanostructured architectures: catalyst-modified carbon−silica composite aerogels. Nano Lett 2:235–240

Boennermann H, Braun G, Brijoux GB, Brinkman R, Tilling AS, Schulze SK, Siepen K (1996) Nanoscale colloidal metals and alloys stabilized by solvents and surfactants Preparation and use as catalyst precursors. J Organomet Chem 520:143–162

Bonnemann H, Richards R (2002) Manufacture of heterogeneous mono- and bimetallic colloid catalysts and their applications in fine chemical synthesis and fuel cells. Synth Methods Organomet Inorg Chem 10:209–224

Boudjahem AG, Monteverdi S, Mercy M, Bettahar MM (2004) Study of nickel catalysts supported on silica of low surface area and prepared by reduction of nickel acetate in aqueous hydrazine. J Catal 221:325–334

Bradley JS (1994) The chemistry of transition metal colloids. In: Schmid G (ed) Clusters and colloids: from theory to applications, chap 6. Wiley-VCH, Weinheim, pp 459–544

Claus P, Hofmeister H (1999) Electron microscopy and catalytic study of silver catalysts: structure sensitivity of the hydrogenation of crotonaldehyde. J Phys Chem B 103:2766–2775

Duff DG, Baiker A (1995) Preparation and structural properties of ultrafine gold colloids for oxidation catalysis. Stud Surf Sci Catal 91:505–512

Gopidas KR, Whitesell JK, Fox MA (2003) Synthesis, characterization, and catalytic applications of a palladium-nanoparticle-cored dendrimer. Nano Lett 3:1757–1760

Henry CR (2000) Catalytic activity of supported nanometer-sized metal clusters. Appl Surf Sci 164:252–259

Jana S, Basu S, Pande S, Ghosh SK, Pal T (2007) Shape-selective synthesis, magnetic properties, and catalytic activity of single crystalline β-MnO_2 nanoparticles. J Phys Chem C 111:16272–16277

Kabir-ud-Din Iqubal SMS (2009) Nanosized MnO_2: preparation, characterisation and its redox activity. Int J Nanoparticles 2:342–349

Kabir-ud-Din Altaf M, Akram M (2008) The kinetics of oxidation of L-tryptophan by water-soluble colloidal manganese dioxide. J Disp Sci Technol 29:809–816

Khan Z, Thabaiti SA, Obaid AY, Khan ZA (2010) MnO_2 nanostructures of different morphologies from amino acids–MnO^{4-} reactions in aqueous solutions. Colloids and Surf B Biointerfaces 81:381–384

Kogan V, Aizenshtat Z, Popovitz-Biro R, Neumann R (2002) Carbon−carbon and carbon−nitrogen coupling reactions catalyzed by palladium nanoparticles derived from a palladium substituted keggin-type polyoxometalate. Org Lett 4:3529–3532

Kralik M, Biffis A (2001) Catalysis by metal nanoparticles supported on functional organic polymers. J Mol Catal A Chem 177:113–138

Kralik M, Corain B, Zecca M (2000) Catalysis by metal nanoparticles supported on functionalized polymers. Chem Pap 54:254–264

Launay F, Roucoux A, Patin H (1998) Ruthenium colloids: A new catalyst for alkane oxidation by tBHP in a biphasic water-organic phase system. Tetrahedron Lett 39:1353–1356

Li Y, El-Sayed MA (2001) The effect of stabilizers on the catalytic activity and stability of Pd colloidal nanoparticles in the Suzuki reactions in aqueous solution. J Phys Chem B 105:8938–8943

Li Y, Boone E, El-Sayed MA (2002) Size effects of PVP−Pd nanoparticles on the catalytic suzuki reactions in aqueous solution. Langmuir 18:4921–4925

Long JW, Stroud RM, Swider-Lyons KE, Rolison DR (2000) How to make electrocatalysts more active for direct methanol oxidation avoid PtRu bimetallic alloys! J Phys Chem B 104:9772–9776

Majetich SA, Jin Y (1999) Magnetization directions of individual nanoparticles. Science 284:470–473

Mayer ABR (2001) Colloidal metal nanoparticles dispersed in amphiphilic polymers. Polym Adv Technol 12:96–106

Moiseev II, Vargaftik MN (2002) Clusters and colloidal metals in catalysis. Russ J Chem 72:512–522

Moore JT, Corn JD, Chu D, Jiang R, Boxall DL, Kenik EA, Lukehart CM (2003) Synthesis and characterization of a Pt3Ru1/Vulcan carbon powder nanocomposite and reactivity as a methanol electrooxidation catalyst. Chem Mater 15:3320–3325

Narayanan R, El-Sayed MA (2003) Effect of catalysis on the stability of metallic nanoparticles: Suzuki reaction catalyzed by PVP-Palladium nanoparticles. J Am Chem Soc 125:8340–8347

Narayanan R, El-Sayed MA (2004a) Effect of nanocatalysis in colloidal solution on the tetrahedral and cubic nanoparticle shape: electron-transfer reaction catalyzed by platinum nanoparticles. J Phys Chem B 108:5726–5733

Narayanan R, El-Sayed MA (2004b) Shape-dependent catalytic activity of platinum nanoparticles in colloidal solution. Nano Lett 4:1343–1348

Nayral C, Viala E, Fau P, Senocq F, Jumas J-C, Maisonnat A, Chaudret B (2000) Synthesis of tin and tin oxide nanoparticles of low size dispersity for application in gas sensing. Chem Eur J 6:4082–4090

Ohde H, Ohde M, Wai CM (2004) Swelled plastics in supercritical CO_2 as media for stabilization of metal nanoparticles and for catalytic hydrogenation. Chem Commun 8:930–931

Puddephatt RJ (1999) Metal clusters in catalysis—an overview. J Met Cluster Chem 2:605–615

Raj K, Moskowitz R (1990) Commercial applications of ferrofluids. J Magn Magn Mater 85:233–245

Sharma RK, Sharma P, Maitra A (2003) Size-dependent catalytic behavior of platinum nanoparticles on the hexacyanoferrate(III)/thiosulfate redox reaction. J Colloid Interf Sci 265:134–140

Shiraishi Y, Toshima N (1999) Colloidal silver catalysts for oxidation of ethylene. J Mol Catal A Chem 141:187–192

Somorjai GA (1997) New model catalysts (platinum nanoparticles) and new techniques (SFG and STM) for studies of reaction intermediates and surface restructuring at high pressures during catalytic reactions. Appl Surf Sci 121(122):1–19

Spiro M, De Jesus D (2000) Nanoparticle catalysis in microemulsions: oxidation of *n*, *n*-dimethyl-*p*-phenylenediamine by cobalt(III) pentaammine chloride catalyzed by colloidal palladium in water/AOT/*n*-heptane microemulsions. Langmuir 16:2464–2468

Thomas JM, Raja R (2001) Nanopore and nanoparticle catalysts. Chem Rec 1:448–466

Thomas JM, Johnson BFG, Raja R, Sankar G, Midgley PA (2003) High-performance nanocatalysts for single-step hydrogenations. Acc Chem Res 36:20–30

Toshima N (1996) Colloidal dispersion of bimetallic nanoparticles: preparation, structure and catalysis. In: Pelizzetti E (ed) Fine particle science and technology, vol 12. NATO ASI Series 3: high technology. Kluwer, Dordrecht, pp 371–383

Toshima N, Yonezawa T (1998) Bimetallic nanoparticles-novel materials for chemical and physical applications. New J Chem 22:1179–1201

Yeung LK, Crooks RM (2001) Heck heterocoupling within a dendritic nanoreactor. Nano Lett 1:14–17

Zarur AJ, Ying JY (2000) Reverse microemulsion synthesis of nanostructured complex oxides for catalytic combustion. Nature 403:65–67